Published in final edited form as:
Pharm Res. 2009 June ; 26(6): 1516–1524. doi:10.1007/s11095-009-9864-8.

Transferrin Receptor Targeted Lipopolyplexes for Delivery of Antisense Oligonucleotide G3139 in a Murine K562 Xenograft Model

Xulang Zhang[1], **Chee Guan Koh**[2], **Bo Yu**[2], **Shujun Liu**[4], **Longzhu Piao**[3], **Guido Marcucci**[4], **Robert J. Lee**[1,3,4,6,7], and **L. James Lee**[1,2,5,7]

[1]NSF Nanoscale Science and Engineering Center (NSEC), The Ohio State University, Columbus, Ohio 43210, USA

[2]Department of Chemical and Biomolecular Engineering, The Ohio State University, Columbus, Ohio 43210, USA

[3]Division of Pharmaceutics, College of Pharmacy, The Ohio State University, Columbus, Ohio 43210, USA

[4]NCI Comprehensive Cancer Center (CCC), The Ohio State University, Columbus, Ohio 43210, USA

[5]140 W 19th Ave., Columbus, Ohio 43210, USA

[6]500 W.12th Ave., Columbus, Ohio 43210, USA

Abstract

Purpose—Transferrin (Tf) conjugated lipopolyplexes (LPs) carrying G3139, an antisense oligonucleotide for Bcl-2, were synthesized and evaluated in Tf receptor positive K562 erythroleukemia cells and then in a murine K562 xenograft model.

Materials and Methods—Particle size and Zeta potentials of transferrin conjugated lipopolyplexs containing G3139 (Tf-LP-G3139) were measured by Dynamic Light Scattering and ZetaPALS. *In vitro* and *in vivo* sample's Bcl-2 downregulation was analyzed using Western blot and tumor tissue samples also exhibited by immunohistochemistry method. For athymic mice bearing with K562 xenograft tumors, tumor growth inhibition and survival rate were investigated. Nanoparticle distribution in 3-D cell cluster was observed by Laser scan confocal microscopy. IL-12 production in the plasma was measured by ELISA kit.

Results—*In vitro*, Tf-LP-G3139 was more effective in inducing down regulation of Bcl-2 in K562 cells than non-targeted LP-G3139, free G3139 and mismatched control ODN-G4126 in the same formulation. *In vivo* Tf-LP-G3139 was less effective than free G3139 in Bcl-2 down regulation. 3-D cell cluster model diffusion results indeed indicated limited penetration of the LPs into the cell cluster. Finally, the therapeutic efficacies of Tf-LP-G3139 and free G3139 were determined in the K562 xenograft model. Tf-LP-G3139 showed slower plasma clearance, higher AUC, and greater accumulation in the tumor compared to free G3139. In addition, Tf-LP-G3139 was found to be more effective in tumor growth inhibition and prolonging mouse survival than free G3139. This was associated with increased spleen weight and IL-12 production in the plasma.

[7]To whom correspondence should be addressed. (Lee.31@osu.edu, Lee.1339@osu.edu).

Conclusion—The role of the immune system in the therapeutic response obtained with the Tf-LPs is necessary and *in vitro* 3-D cell cluster model can be a potential tool to evaluate the nanoparticle distribution.

Keywords

Bcl-2; leukemia; lipopolyplexs; targeted drug delivery; transferrin receptor

INTRODUCTION

Acute myelogenous leukemia (AML) is the most common type of adult leukemia. For most AML subtypes, current therapy has only limited efficacy, partly due to amplified expression of the B-cell leukemia/lymphoma 2 (Bcl-2) protein, which makes leukemia cells resistant to apoptosis (1). To overcome Bcl-2 related drug resistance, an antisense oligonucleotide (ODN), G3139 (oblimersen, Genasense™), has been developed as a Bcl-2 down-regulating agent. G3139 is an 18-mer phosphorothioate ODN complementary to codons 1–6 of the Bcl-2 mRNA (2). An antisense ODN hybridizes with the target mRNA and forms a heteroduplex that activates RNase H, which degrades the mRNA. This results in the down regulation of the target gene. Because ODNs are of high molecular weight and are polyanionic agents, they lack an efficient mechanism to cross the cellular membrane. Free ODNs have shown relatively poor intracellular bioavailability both *in vitro* and *in vivo* (3). Possibly as a result, G3139 failed to show significant clinical efficacy in a recent Phase III trial in AML patients (4,5).

Transferrin receptor (TfR) targeted lipopolyplexes (LPs) have been shown to improve the delivery of G3139 to human erythroleukemia K562 cells, which overexpress TfR. Tf is an iron transport protein that, when associated with ferric ion, binds with high affinity to TfR, which is overexpressed frequently on leukemia cells (6). According to recently reported studies in our group, Tf-LP G3139 has an advantage over non-Tf-LP G3139 in K562 cellular uptake (7). In this study, Tf-conjugated LPs carrying G3139 were characterized in a K562 subcutaneous xenograft model in athymic mice and studied for Bcl-2 down regulation and tumor inhibitory activity. We found that, with respect to Bcl-2 down regulation, *In vivo* data did not correlate with *in vitro* findings. The role of intratumoral diffusion in target downregulation was investigated in a 3-D cell cluster model. The potential implication of the findings in nanoparticle based drug delivery is discussed.

MATERIALS AND METHODS

Materials

Egg phosphatidylcholine (egg PC), 3β-[*N*-(*N*,*N*-dimethylaminoethane)-carbamoyl] cholesterol hydrochloride (DC-Chol) and maleimido-polyethyleneglycol (M.W. ~2,000)—distearoylphosphatidylethanolamine (Mal-PEG-DSPE) were purchased from Avanti Polar Lipids (Alabaster, AL). Methoxy-PEG_{2000}-DSPE (PEG-DSPE) was purchased from Genzyme Corporation (Cambridge, MA). Human holo-transferrin (Tf), 2-iminothiolane (Traut's reagent), protamine sulfate, and other chemical reagents were purchased from Sigma Chemical Co. (St. Louis, MO). All tissue culture media and supplies were purchased from Invitrogen (Carlsbad, CA). All ODNs used in this study were fully phosphorothioated. Antisense ODN G3139 (5′-TCT CCC AGC GTG CGC CAT-3′) and its fluorescence-labeled derivative, fluorescein isothiocyanate FITC-G3139 (G4243) and mismatched control ODN G4126 (5′-TCT CCCAGCATG TGC CAT-3′) were generously provided by Genta Inc. (Berkeley Heights, NJ).

Synthesis of TfR-targeted Lipopolyplexes (Tf-LPs) Loaded with ODN

LPs composed of a lipid mixture (egg PC/DC-Chol/DSPE-PEG at a molar ratio of 65:30:2), protamine, and ODN (G3139, its fluorescent derivative G4243, or mismatched control G4126) were prepared by an ethanol dilution method, as described previously (8). Briefly, the lipid mixture was dissolved in 100% ethanol (EtOH) and mixed with protamine sulfate in sodium citrate buffer (20 mM, pH 4.0) to achieve an EtOH concentration of 66.6% (*v*/*v*). ODN (1.33 mg/ml) in sodium citrate buffer (20 mM, pH 4.0) was then added to lipid-protamine solution under vortexing to spontaneously form pre-LPs at an EtOH concentration of 40% (*v*/*v*) (1 μg ODN:12.5 μg lipids). The complexes were then dialyzed against sodium citrate buffer (20 mM, pH 4) at room temperature for 1 h and then against 1× PBS (pH 7.4) overnight at room temperature, using a Spectropore Float-A-Lyzer (Spectrum Labs, Rancho Dominguez, CA) with a Molecular Weight Cut-Off of 10,000 Da to raise the pH so as to partially neutralize the DC-Chol. This will yield non-targeted LPs. Tf ligand was then incorporated into the ODN-loading LPs using a post insertion method to form Tf-LP G3139 (9). Briefly, holo(diferric)-transferrin (holo-Tf) in 1× phosphate-buffered saline (PBS, pH=8) was mixed with 5× Traut's reagent to yield thiolated Tf (holo-Tf-SH). Free Traut's reagent was removed through a D-Salt Dextran Desalting Column (Pierce, Rockford, IL) with 1× phosphate-buffered saline (PBS, pH=6.5) using a protein assay (Bio-Rad) to detect Tf in the elution. Next, holo-Tf-SH was then reacted with micelles of Mal-PEG-DSPE at a protein-to-lipid molar ratio of 1:10 for 2 h at room temperature in 1× PBS (pH=6.5) and dialyzed using a SpectraPor Float-A-Lyzer MWCO 5,000 Dalton (Spectrum Labs, Rancho Dominguez, CA) against 1× PBS (pH=7.4) to form Tf-PEG-DSPE. For incorporating Tf ligand into ODN-loaded LPs, ODN-loaded LPs were incubated with Tf-PEG-DSPE for 1 hr at 37°C at a Tf-PEG-DSPE-to-LP lipid ratio of 1:100 (1 mol% based on DSPE-PEG) to generate Tf-LPs (Tf/LPs=80 μg/1 μ mol).

Characterization of the Tf-LPs

Particle size distribution and zeta potentials (ζ) of the LPs were analyzed in citrate buffer (pH=4) on BI-200SM and ZetaPALS (Brookhaven Instruments Corp., Holtsville, NY), respectively. For particle sizing, LP samples at a concentration of 25 μg/500 μl PBS were used. Volume-weighted Gaussian distribution analysis was used to determine the mean LP diameter. All the measurements were carried out in triplicate immediately after the preparation of the LPs.

Analysis of ODN in LPs

To analyze their ODN content, LPs were analyzed by gel electrophoresis before and after lysis in 1% SDS. About 20 μg LPs in PBS buffer were loaded onto a 3% ReadyAgarose™ gel containing ethidium bromide (Bio-Rad Laboratories, Hercules, CA). Electrophoresis was carried out at 100 V for 30 min in a 1× TAE buffer (Invitrogen). A digital image of the gel was captured under UV light using ChemiDoc XRS system (Bio-Rad).

Cell Culture

Human erythroleukemia cell line K562 was purchased from American Type Culture Collection (ATCC) (Manassas, VA). The cells were maintained in RPMI-1640 media supplemented with 10% heat-inactivated fetal bovine serum (FBS), 100 U/mL penicillin, 100 μg/mL streptomycin, and L-glutamine. Cells were cultured at 37°C in a humidified atmosphere containing 5% CO_2.

In Vitro K562 Cells Transfection

K562 cells were plated in 6-well tissue culture plates at 10^6/well in 1.2 mL RPMI1640 medium containing 10% FBS. Appropriate amount of liposomal formulations (Tf-LP

G3139, non Tf-LP G3139 and Tf-LP G4126) were added into each well to yield a final ODN concentration of 1 μM and the cells were then incubated at 37°C in a CO_2 incubator for 6 h. The cells were then transferred to fresh medium, incubated for a further 48 h, and then analyzed for Bcl-2 protein level by Western blot.

Animals

Female athymic mice (HSD:Athymic nude-FOXN1nd) and ICR mice were purchased from Harlan (Indianapolis, IN) and Taconic (Hudson, NY), respectively. All mice were 6–8 weeks of age at the time of arrival. All animal experiments were approved by the Institutional Animal Care and Use Committee (IACUC) at The Ohio State University.

In vivo Plasma Clearance

For plasma clearance studies, free ODN (G4243 = FITC labeled G3139), and Tf-LPs containing the same ODNs were administered via tail vein injection into ICR mice at 5 mg/kg (n = 5) (10,11). At appropriate time points, mice were anesthetized and blood was collected via tail vein by using heparinized tubes. Plasma was separated from red blood cells via immediate centrifugation at 10,000×g for 5 min. SDS was then added to obtain a final concentration of 1% in a volume of 500 μL. The samples were heated to 95°C for 5 min, followed by centrifugation at 12,000×g for 5 min. The fluorescence of supernatant was determined on a spectrofluorometer (PerkinElmer, Boston, MA). Mice were sacrificed by carbon dioxide inhalation.

G3139 Accumulation in Tumor

K562 cells (1×10^7/100 μl) were subcutaneously (s.c.) inoculated into the right flank of athymic mice. Tumor-bearing mouse was injected with 5 mg/kg ODN (ODN concentration: 1 mg/ml; n=5) via tail vein when tumor size reached 50 mm^3. Tumors were harvested at 36 h post injection and homogenized in micro tubes containing 450 μL distilled water. SDS was then added to obtain a final concentration of 1% in a volume of 500 μL. The samples were heated to 95°C for 5 min, followed by centrifugation at 12,000×g for 5 min. The fluorescence of supernatant was determined on a spectrofluorometer (PerkinElmer, Boston, MA).

Anti-tumor Activity of Tf-LP G3139 in Murine Xenografts

K562 cells (1×10^7/100μl) were subcutaneously (s.c.) inoculated into the right flank of athymic mice. When tumors developed and reached a mean volume of approximately 50 mm^3, the mice were separated into four groups and were untreated or treated with free ODN (G3139, 5 mg/kg), Tf-LP mismatched ODN (Tf-LP G4126, 5 mg/kg) or Tf-LP G3139 (5 mg/kg dose of ODN) every other day starting on day 7 for a total of 700 μg treatments. Mouse body weight and tumor volume were monitored every day. Tumor dimensions were measured by a vernier caliper and calculated using the formula: $A\times B^2/2$, where A and B are perpendicular axes and represent the longest and shortest dimensions, respectively. Mice were sacrificed upon the tumor size exceeding 1,500 mm^3 per early removal criteria. Each treatment group comprised five animals.

Immunohistochemistry (IHC) Staining of the Tumor

For histochemical analysis, tumor samples were fixed with 4% buffered formalin and subsequently embedded in paraffin and sectioned using a microtone. After mounting onto slides, the samples were deparaffinized and treated with 3% hydrogen peroxide in methanol. The tissues were then rinsed three times with PBS and blocked for 2 h at room temperature with 1% normal goat serum in PBS. Primary antibody rabbit anti-Bcl-2 (Santa Cruz Biotechnology) at 1:200 dilution was added onto the slide, followed by overnight incubation

at 4°C. The slides were then washed three times with PBS, treated with biotinylated anti-rabbit IgG and incubated at room temperature for 1 h. Finally, the samples were counterstained with hematoxylin and eosin (H&E), dehydrated, and mounted with Permount. Slides with H&E staining only were used as control.

Quantification of Bcl-2 Protein Level by Western Blot

The Western blot was carried out to evaluate the Bcl-2 protein in tumor tissues from mice and in K562 cells or clusters. Briefly, 15~20 mg of tumor tissue was homogenized in 0.6 ml lysis buffer containing a protease inhibitor cocktail (CalBiochem, San Diego, CA) using a homogenizer. Tissue or K562 cells cluster with lysis buffer were incubated on ice for 20 min followed by centrifugation of the cell lysate at 14,000×*g* at 4°C for 10 min. Then the supernatants were collected and the protein concentrations were determined by BCA assay (Pierce, Rockford, IL). Then, 100 μg protein from each sample was loaded onto a 15% Ready Gel Tris–HCl polyacrylamide gel (Bio-Rad, Hercules, CA) for 2 h at 100 V, followed by transfer of the proteins to a PVDF membrane overnight. After blocking with 5% non-fat dry milk in 1× Tris-buffered saline/Tween-20 (TBST) for 1 h, the membranes were incubated with monoclonal mouse anti-human Bcl-2 (Dako, Carpinteria, CA) or polyclonal goat anti-human β-actin antibody (Santa Cruz, Santa Cruz, CA). After 2 h of incubation at room temperature, the membranes were washed four times (15 min each) with TBST, followed by incubation with horseradish peroxidase-conjugated sheep anti-mouse IgG (Amersham Biosciences, Piscataway, NJ) or rabbit anti-goat IgG (Pierce, Rockford, IL) for 1 h at room temperature. Membrane was then developed with Pierce SuperSignal West Dura Extended Duration Substrate (Pierce, Rockford, IL) and imaged with Kodak X-OMAT film (Kodak, Rochester, NY) by X-ray. Prior to beta actin incubation, the membranes were stripped and blocked. Bcl-2 protein expression levels were quantified by ImageJ software (NIH Image, Bethesda, MD) and normalized to the β-actin level from the same sample.

Measurement of IL-12 Production

For detection of serum IL-12, blood samples were collected from the tail vein of the nude mice at various time points following treatment with Tf-LP G4126, free G3139, and Tf-LP G3139. After incubation at room temperature for 30 min, blood samples were collected and centrifuged at 12,000×*g* to obtain serum. The level of cytokine was determined by ELISA using a commercial kit for IL-12 (BD Pharmingen, San Diego, CA). Spleen was harvested from nude mice after sacrifice and weighed. Each group included 5 mice.

K562 Cells Cluster Preparation

K562 cells cluster were prepared by a microencapsulation method using alginate and poly-L-lysine (AP). AP microcapsules entrapping K562 cells were prepared as described previously with minor modification (12). Briefly, cells were suspended in 1.5% *w/v* sterilized sodium alginate (Sigma, St. Louis, MO) and extruded into 100 mM $CaCl_2$ using an electrostatic droplet generator to form calcium alginate gel beads. The gel beads were incubated with 0.05% *w/v* poly-L-lysine (*M*w 65,000; Sigma, St. Louis, MO) to form alginatepoly-L-lysine membrane. The membrane-enclosed gel beads were further suspended in 55 mM sodium citrate to liquefy the alginate gel core, resulting in AP microcapsules that were 250–350 μm in diameter. The microcapsules with K562 cells were cultured at 37°C and in 5% CO_2 in RPMI-1640 medium supplemented with 10% FBS. K562 cells proliferated and formed 150 μm in diameter cells clusters after 6 days in culture. The diameter of cell cluster was close to the diffusion length between capillary vessels.

Diffusion and Bcl-2 Downregulation by Free ODN and Tf-LP ODN Inside K562 Cell Clusters

K562 cell clusters were treated with G3139 spiked with 10% fluorescent G4243 or Tf-LPs containing the same amount of G3139 or G4243. The concentrations of ODN used were adjusted according to the amount of G3139 that was accumulated in tumor tissue in the above described *in vivo* studies of the xenograft model. A mechanical method was used for removing the enclosing membrane of microcapsule. Tf-LPs containing G3139 was used in the bcl-2 downregulation test and Tf-LPG4243 in the ODN diffusion test. K562 cells clusters (10^6/well) were incubated with free ODN or Tf-LPs ODN (1 μM ODN final concentration) for 6 hr, rinsed, cultured overnight in fresh culture medium and then fixed with 4% paraformaldehyde. The cell's cytoplasm and nucleus were stained by DiI Cell-Tracker (Invitrogen/Molecular Probes) and DRAQ5 (Biostatus Limited, Leicestershire, United Kingdom), respectively. Finally, K562 cells clusters were mounted with Prolong Gold antifade reagent (Invitrogen, Eugene, Oregon, USA) and observed under laser scan confocal microscopy (510 Meta CLSM, Zeiss, Germany) with excitation wavelengths of 488 nm and 543 nm for G4243 and DiI, respectively. This was performed at The Ohio State University's Campus Microscopy and Imaging Facility (CMIF).

Statistical Analysis

Data were presented as means and standard deviations (S.D.) and were analyzed by a two-tailed Student's *t*-test using MiniTAB software (Minitab Inc., State College, PA). Survival rate was assayed by log rank test. $p<0.05$ was considered statistically significant.

RESULTS

Particle Size, Zeta Potential and G3139 Encapsulation

The size and zeta potential values of particles at various stages of LP synthesis are analyzed. The dialysis steps reduced the particle size and zeta potential of LP G3139 from 315.5±3.7 nm and 35.4±0.4 mV to 126.8±2.2 nm and 11.6±3.6 mV, respectively. Incorporation of Tf into LPs slightly increased the particle size to 141.3±2.0 nm and reduced the zeta potential to 3.6±2.9 mV. Each data represents mean±standard deviation of three separate experiments (Table I). G3139 has been successfully encapsulated into LPs as determined by gel electrophoresis (data not shown).

In vitro Bcl-2 Downregulation of K562 Cells

The efficiency of targeted delivery of G3139 nanoparticles was evaluated by the expression of Bcl-2 protein levels in K562 leukemia cell line *in vitro*. As shown in Fig. 5a, Tf-LP G3139 is resulted in the greatest reduction with Bcl-2 protein levels in K562 cells as compared to free G3139, non-targeted liposomes G3139 and Tf-LP containing mismatched ODN, respectively.

Pharmacokinetic Study

Pharmacokinetic studies in ICR mice were performed to evaluate the circulation time of the Tf-LP ODN, as shown in Fig. 1. Pharmacokinetic parameters were calculated with WinNonlin software (Scientific Consulting, Inc., Apex, N.C.) using two compartmental analysis (Table II). Tf-LP ODN i.v. administered to mice at 5 mg/kg resulted in a peak plasma concentration (C_{max}) and an elimination phase half-life ($t_{1/2}$) of 29.3 μg/mL and 8.49 h, respectively. The area under the plasma concentration time curve (AUC) was 90.02 h•μg/mL. In contrast, the same amount of free G4243 i.v. administered to mice yielded a C_{max} and a terminal half-life ($t_{1/2}$) of 61.1 μg/mL and 0.63 h, respectively, indicating that the free G4243 was rapidly cleared from circulation. The AUC was only 9.32 h•μg/mL.

G3139 Concentration in Tumor Tissue

Due to the improvement in serum stability (data not shown), prolong circulation time and the associated enhanced permeability and retention (EPR) effect, and TfR mediated uptake. Tf-LP loaded ODN was delivered into solid tumors more efficiently than free ODN. As shown in Fig. 2, 2.4-fold higher G3139 concentration was found in tumor tissue following Tf-LP administration compared with tumors treated with free G3139.

Tf-LP G3139 Inhibited Tumor Growth

The *in vivo* antitumor efficacy of G3139 was evaluated in a K562 tumor bearing athymic mouse model. Free and Tf-LP G3139 were administered by i.v. injection via tail vein. Antitumor activity was determined by measuring the tumor volume and monitoring animal survival. As shown in Fig. 3a, tumor growth in the mice treated with Tf-LP G3139 was suppressed significantly, resulting in prolonged survival in 60% of mice (three out of five) with a median survival of 40 days whereas mice treated with G3139 alone showed less efficacy (Fig. 3b). The treatment group/control group survival time ratio (%T/C) value of 147, 194 for the free G3139 and Tf-LP G3139 groups suggested that Tf-LP G3139 was much more effective in prolonging the survival of tumor bearing mice.

In vivo Downregulation of Bcl-2 by Tf-LP G3139

The efficiency of targeted delivery of Tf-LP G3139 was evaluated by Bcl-2 protein expression levels in tumor tissue. As shown in Fig. 4, immunohistochemical staining for Bcl-2 protein, as indicated by brown color, in the cytoplasm of K562 cell in tumor xenograft tissue demonstrated downregulation of Bcl-2 protein expression in both free G3139 and Tf-LP G3139 treatment groups. However, it is difficult to quantify the degree of Bcl-2 downregulation based on these images. Therefore, Western blot for Bcl-2 protein level was performed. As shown in Fig. 5b, free G3139 treated tumors expressed lower amount of Bcl-2 protein as compared to the Tf-LP G3139 treated group. This indicated that free G3139 can more efficiently down regulate Bcl-2 protein expression in K562 engrafted tumor than the Tf-LP G3139.

Immunostimulatory Effects of Tf-LP G3139 in Nude Mice

Nucleic acids containing CpG motifs are known to stimulate innate immune responses via toll-like receptor 9 (TLR9) activation (13–15). G3139 contains 2 CpG motifs and have been shown to trigger TLR9 activation. Plasma interleukin 12 (IL-12) is a useful indicator of TLR9 activation (16). Serum level of IL-12 in tumor-bearing mice was determined by ELISA at 8 h after treatment. As shown in Fig. 6 (a), only low levels of IL-12 were detected in the sera of mice treated with free G3139 or the mismatched ODN G4126. Meanwhile, the IL-12 level was much higher in the Tf-LP G3139 treatment group. The results suggest that the antitumor activity of Tf-LPs might be associated with their potential capacity to induce cytokine production. In addition to elevated IL-12 production, Tf-LP treatment also resulted in a significant enlargement of the spleens as compared to those mice treated with free G3139 or Tf-LP G4126 (Fig. 6b) on day 15.

In vitro Bcl-2 Downregulation in K562 Cells Clusters

K562 cells clusters were used as an *in vitro* model for studying diffusion of ODN and LPs in a 3-D tissue environment. The K562 cells clusters were treated with free G3139 and Tf-LP G3139 at the same concentrations as those found in the tumor tissues. As shown in Fig. 5 (c), free G3139 treatment group demonstrated more Bcl-2 downregulation than the Tf-LP treatment group. This was consistent with the *in vivo* results obtained in the K562 xenograft model. This indicated that even though more G3139 was delivered to the tumor tissue *in vivo* by Tf-LP, the nanoparticles had limited capacity to diffuse into the K562 cells in a 3-D

environment. The correlation of transfection results in the 3-D cell cluster and *in vivo* suggest that the 3-D cell cluster closely resembled animal tumor and may be a useful model system for modeling tumor drug delivery.

FITC-labeled G3139 Distribution in K562 Cells Cluster

As shown in Fig. 7, free ODN diffused into inner layer of the cells cluster easily due to their small size. Green dots of free G4243 (G4243: FITC-labeled G3139) were located in the inter- and intracellular areas of the cluster. ODN was found even in the deep layers in the cell cluster as shown in Fig. 7a. In contrast, G4243 delivered by Tf-LP only was seen in the outermost layers but not the inner layer of cells cluster (Fig. 7b). This indicated little amount of G4243 was released from nanoparticle and diffused into inner layer of cell clusters. The greater abundance of G4243 found in the cluster in the free ODN treated group might explain the better Bcl-2 downregulation in both *in vitro* cells cluster and in animal tumor model.

DISCUSSION

This paper demonstrated that encapsulating G3139 into lipid nanoparticles prolongs its circulation time and enhanced the antitumor effect, possibly by the combined effects of Bcl-2 downregulation and immunostimulation. Meidan *et al.* (14) presented the polyplexs formulation of DC-Chol/DOPC/CCS for G3139 delivery and showed efficient down regulation of Bcl-2 in the MCF-7 cell line. In our previous *in vitro* study (9), it was demonstrated that liposomal formulation (DC-Chol/egg PC/DSPE-PEG) conjugated with Tf as a targeting ligand enhanced the antisense activity of G3139 in K562 cells. In this study, a similar formulation with a lower amount of DSPE-PEG but also included protamine was used to produce LPs with long circulation time and high ODN encapsulation efficiency. G3139 formulated in our liposomes exhibited a much greater AUC and longer half-life, resulting in better inhibition of tumor growth and longer survival rate as compared to free G3139 *in vivo*.

K562 human tumor xenografts in nude mice were first used in our study and Tf-LP G3139 showed greater activity in tumor inhibition than free G3139 in prolonging animal survival. Tf-LP G4126, which contained a mismatched ODN, did not show significant Bcl-2 down regulation and immune effect in K562 xenografts model, possibly due to the sequence mismatch and the lack of CpG motifs in G4126. The antitumor effect observed in K562 human tumor xenografts in nude (immunocompromised) mice was possibly mediated by Bcl-2 gene downregulation as well as by CpG-modulated immune response since both mechanisms have been reported previously (17). Recently, Pan *et al.* (18) reported that similar LPs loaded with G3139 were much more therapeutically active than free G3139 in inhibiting the growth of murine L1210 tumors in DBA/2 (immunocompetent) mice. In that study, no down regulation of murine bcl-2 was found and the enhanced antitumor activity was attributed to immunomodulatory effects due to TLR9 activation. In the current study, an athymic mouse model, which is immunosuppressed, was used and K562, which is a human cell line, formed the tumor. The results nonetheless seemed to suggest that the immunomodulatory effects of G3139-LPs rather than (or in addition to) Bcl-2 downregulation was likely responsible for the observed antitumor activity. Tf-LPs containing ODNs mediated greater ODN delivery into solid tumors as compared to the same dose of free ODN. However, it was the free G3139 that showed greater Bcl-2 down-regulation. This might be because LPs' large size limited their diffusion inside the solid tumor resulting in distribution only to the cell layers close to the blood vessel. Since free G3139 molecules are smaller in size, they can readily diffuse into additional cells layers. Therefore, intratumoral diffusion is an important limiting factor in antisense ODN's pharmacological activity. The difference in G3139 diffusivity in the tumor tissue was further

demonstrated by culturing K562 cells into a 3-D pattern that mimics a solid tumor. Using confocal microscopy, we demonstrated that higher amounts of G4243 were found in the inner layers of K562 cells cluster when they were treated with free ODN as compared to when they were treated with the Tf-LP. The greater distribution of free G3139 might have resulted in better Bcl-2 downregulation both in *in vitro* cells cluster and in the solid tumor.

A number of recent studies have also shown enhanced immunostimulatory activities upon CpG ODN loading into liposomes (19,20). The precise mechanism underlying this enhancement remains elusive. One possible mechanism for this enhancement could be that loading ODN into nanoparticles such as liposomes could enhance uptake of the ODN by macrophages and dendritic cells, which are critical to immune activation (21). Interleukin 12 (IL-12) is an cytokine that is naturally produced by dendritic cells (22), macrophages and human B-lymphoblastoid cells in response to antigenic stimulation. In this study, IL-12 was found at relatively high levels in the Tf-LP G3139 group. The reasons we believe are the following: In our formulation, the Tf in the LPs could also target macrophages, which are TfR expressing and have a natural propensity to take up nanoparticles; on the other hand, CpG DNA is known to increase the production of proinflammatory and Th1 cytokines (including IL-12, IL-6 and IFN-γ) (23). Evidence has indicated that spleen was enlarged and its weight increased. It has been reported that tumor cells undergoing necrosis can stimulate spleen cells to produce large amounts of IFN-γ (24). The empty Tf liposome vector did not show significant immune effect in our study.

Another interesting observation in this study was that the Tf-LP G3139 was more efficient at inhibiting tumor growth than free G3139 in despite of lower Bcl-2 down regulating activity. It is likely that the CpG mediated immunological effects more than compensated for the reduced Bcl-2 down regulating activity of the Tf-LPs, consistent with recent findings by Pan *et al.* in the immunocompetent syngenic murine tumor model.

CONCLUSION

A TfR targeted LP formulation for ODN delivery was synthesized and characterized. The Tf-LPs delivered much more G3139 to tumor tissue then free ODN but was less effective in Bcl-2 down regulation, possibly due to limited LP distribution in the tumor. K562 grown as 3-D cells clusters can mimic solid tumor *in vivo* in demonstrating the greater diffusion rate of G4243 relative to the Tf-LPs. Further research will focus on the refinement of the LP formulation and improve the release rate of ODN in targeted tissue to achieve greater Bcl-2 down regulation efficiency.

Acknowledgments

This work was support in part by NSF grant EEC-0425626 and NIH grant R01 CA135243 and R21 CA131832. We wish to thank Genta Inc. for providing us with the ODNs G3139 and G4243.

ABBREVIATIONS

AML	Acute myelogenous leukemia
AUC	Area under the plasma concentration *versus* time curve
Bcl-2	B-cell leukemia/lymphoma 2 protein
DC-Chol	3β-[*N*-(*N*, *N*-dimethylaminoethane)-carbamoyl] cholesterol hydrochloride
egg PC	Egg phosphatidylcholine

EPR	Enhanced permeability and retention
EtOH	Ethanol
H&E	Hematoxylin and eosin
LPs	Lipopolyplexes
Mal-PEG-DSPE	Maleimide-polyethyleneglycol (M.W. ~2000)–distearoylphosphatidylethanolamine
PEG-DSPE	Methoxy-PEG_{2000}-DSPE
TBST	Tris-buffered saline/Tween-20
Tf	Transferrin
TfR	Transferrin receptor
Tf-LP-G3139	Transferrin conjugated lipopolyplexs containing G3139

REFERENCES

1. Reed JC. Bcl-2 family proteins: regulators of apoptosis and chemoresistance in hematologic malignancies. Semin Hematol. 1997; 34(4 Suppl 5):9–19. [PubMed: 9408956]
2. Lopes D, Mayer LD. Pharmacokinetics of Bcl-2 antisense oligonuleotide (G3139) combined with doxorubicin in SCID mice bearing human breast cancer solid tumor xenografts. Cancer Chemother Pharmacol. 2002; 49:57–68. [PubMed: 11855753]
3. Shi F, Visser WH, de Jong NM, Liem RS, Ronken E, Hoekstra D. Antisense oligonucleotides reach mRNA targets via the RNA matrix: downregulation of the 5-HT1A receptor. Exp Cell Res. 2003; 291:313–325. [PubMed: 14644154]
4. Del Poeta G, Bruno A, Del Principe MI, Venditti A, Maurillo L, Buccisano F, Stasi R, Neri B, Luciano F, Siniscalchi A, de Fabritiis P, Amadori S. Deregulation of the mitochondrial apoptotic machinery and development of molecular targeted drugs in acute myeloid leukemia. Curr Cancer Drug Targets. 2008; 8:207–222. [PubMed: 18473734]
5. Moreira JN, Santos A, Simões S. Bcl-2-targeted antisense therapy (Oblimersen sodium): towards clinical reality. Rev Recent Clin Trials. 2006; 1:217–235. [PubMed: 18473975]
6. Sato Y, Yamauchi N, Takahashi M, Sasaki K, Fukaura J, Neda H, Fujii S, Hirayama M, Itoh Y, Koshita Y, Kogawa K, Kato J, Sakamaki S, Niitsu Y. *In vivo* gene delivery to tumor cells by transferrin-streptavidin-DNA conjugate. FASEB J. 2000; 14:2108–2118. [PubMed: 11023995]
7. Yang X, Koh CG, Liu S, Pan X, Santhanam R, Yu B, Peng Y, Pang J, Golan S, Talmon Y, Jin Y, Muthusamy N, Byrd JC, Chan KK, Lee LJ, Marcucci G, Lee RJ. Transferrin Receptor-Targeted Lipid Nanoparticles for Delivery of an Antisense Oligodeoxyribonucleotide against Bcl-2. Molecular Pharmaceutics. Publication Date (Web): December 15, 2008.
8. Xu L, Pirollo KF, Tang WH, Rait A, Chang EH. Transferrin-liposome-mediated systemic p53 gene therapy in combination with radiation results in regression of human head and neck cancer xenografts. Hum Gene Ther. 1999; 10:2941–2952. [PubMed: 10609655]
9. Chiu SJ, Liu S, Perrotti D, Marcucci G, Lee RJ. Efficient delivery of a Bcl-2-specific antisense oligodeoxyribonucleotide (G3139) via transferrin receptor-targeted liposomes. J Control Release. 2006; 112:199–207. [PubMed: 16564596]
10. Xiang G, Wu J, Lu Y, Liu Z, Lee RJ. Synthesis and evaluation of a novel ligand for folate-mediated targeting liposomes. Int J Pharm. 2008; 356:29–36. [PubMed: 18258394]
11. Hussain MM, Maxfield FR, Mas-Oliva J, Tabas I, Ji ZS, Innerarity TL, Mahley RW. Clearance of Chylomicron Remnants by the Low Density Lipoprotein Receptor-related Protein/α2 -Macroglobulin Receptor. J. Biol. Chem. 1991; 266:13936–13940. [PubMed: 1713211]
12. Ma X, Vacek I, Sun A. Generation of alginate-poly-l-lysine-alginate (APA) biomicrocapsules: the relationship between the membrane strength and the reaction conditions, Artificial Cells, Blood Substitutes. Immobilization Biotechnol. 1994; 22:43–69.

13. Krieg AM. CpG motifs in bacterial DNA and their immune effects. Annu Rev Immunol. 2002; 20:709–760. [PubMed: 11861616]

14. Meidan V, Glezer J, Salomon S, Sidi Y, Barenholz Y, Cohen JS, Lilling G. Specific Lipoplex-Mediated Antisense Against Bcl-2 in Breast Cancer Cells: A Comparison between Different Formulations. Journal of Liposome Research. 2006; 16:27–43. [PubMed: 16556548]

15. Krieg AM. CpG motifs: the active ingredient in bacterial extracts? Nat Med. 2003; 9:831–835. [PubMed: 12835699]

16. Shankaran V, Ikeda H, Bruce AT, White JM, Swanson PE, Old LJ, Schreiber RD. IFNgamma and lymphocytes prevent primary tumour development and shape tumour immunogenicity. Nature. 2001; 410:1107–1111. [PubMed: 11323675]

17. Gekeler V, Gimmnich P, Hofmann H-P, Grebe C, Rommele M, Leja A, Baudler M, Benimetskaya L, Gonser B, Pieles U, Maier T, Wagner T, Sanders K, Beck JF, Hanauer G, Stein CA. G3139 and other CpG-Containing Immunostimulatory Phosphorothioate Oligodeoxynucleotides are Potent Suppressors of the Growth of Human Tumor Xenografts in Nude Mice. Ologonucleotides. 2006; 16:83–93.

18. Pan X, Chen L, Liu S, Yang X, Gao J, Lee RJ. Antitumor Activity of G3139 Lipid Nanoparticles (LNPs). Mol Pharm. 2009; 6:211–220. [PubMed: 19072654]

19. Suzuki Y, Wakita D, Chamoto K, Narita Y, Tsuji T, Takeshima T, Gyobu H, Kawarada Y, Kondo S, Akira S, Katoh H, Ikeda H, Nishimura T. Liposome-Encapsulated CpG oligodeoxynucleotides as a potent adjuvant for inducing type 1 innate immunity. Cancer Res. 2004; 64:8754–8760. [PubMed: 15574787]

20. Li WM, Bally MB, Schutze-Redelmeier MP. Enhanced immune response to T-independent antigen by using CpG oligodeoxynucleotides encapsulated in liposomes. Vaccine. 2001; 20:148–157. [PubMed: 11567759]

21. Mui B, Raney SG, Semple SC, Hope MJ. Immune stimulation by a CpG containing oligodeoxynucleotide is enhanced when encapsulated and delivered in lipid particles. J Pharmacol Exp Ther. 2001; 298:1185–1192. [PubMed: 11504819]

22. Kaliński P, Hilkens CM, Snijders A, Snijdewint FG, Kapsenberg ML. IL-12-deficient dendritic cells, generated in the presence of prostaglandin E2, promote type 2 cytokine production in maturing human naive T helper cells. J. Immunol. 1997; 159:28–35. [PubMed: 9200435]

23. Klnman DM, Yi AK, Beaucage SL, Conover J, Krieg AM. CpG motifs present in bacteria DNA rapidly induce lymphocytes to secrete interleukin 6, interleukin 12, and interferon γ. Proc. Natl. Acad. Sci. USA. 1996; 93:2879–2883. [PubMed: 8610135]

24. Smyth MJ, Godfrey DI, Trapani JA. A fresh look at tumor immnosurveillance and immunotherapy. Nat. Imunol. 2001; 2:293–299.

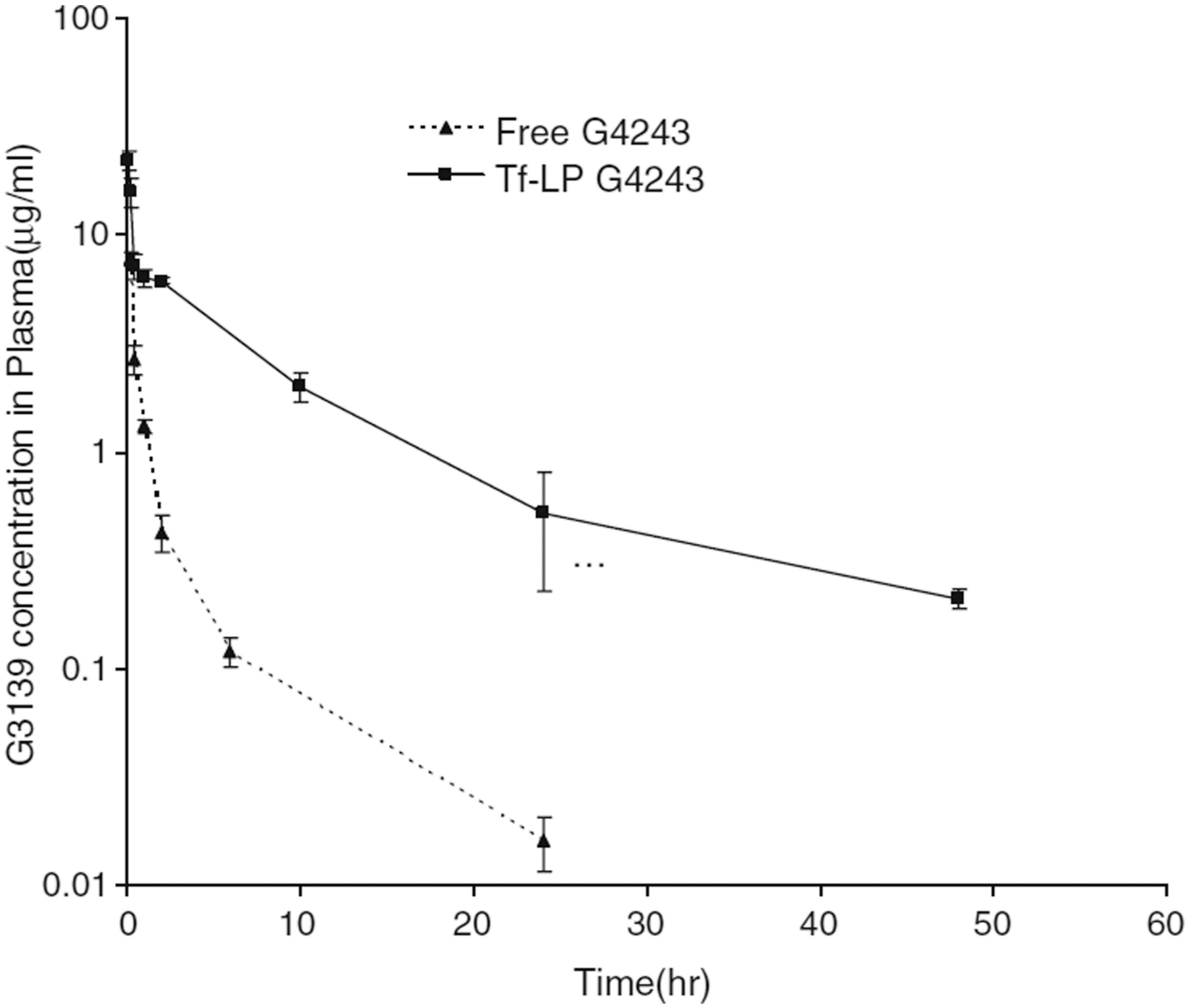

Fig. 1.
Plasma clearance of Tf-LP G4243 and free G4243 in ICR mice (n=5).

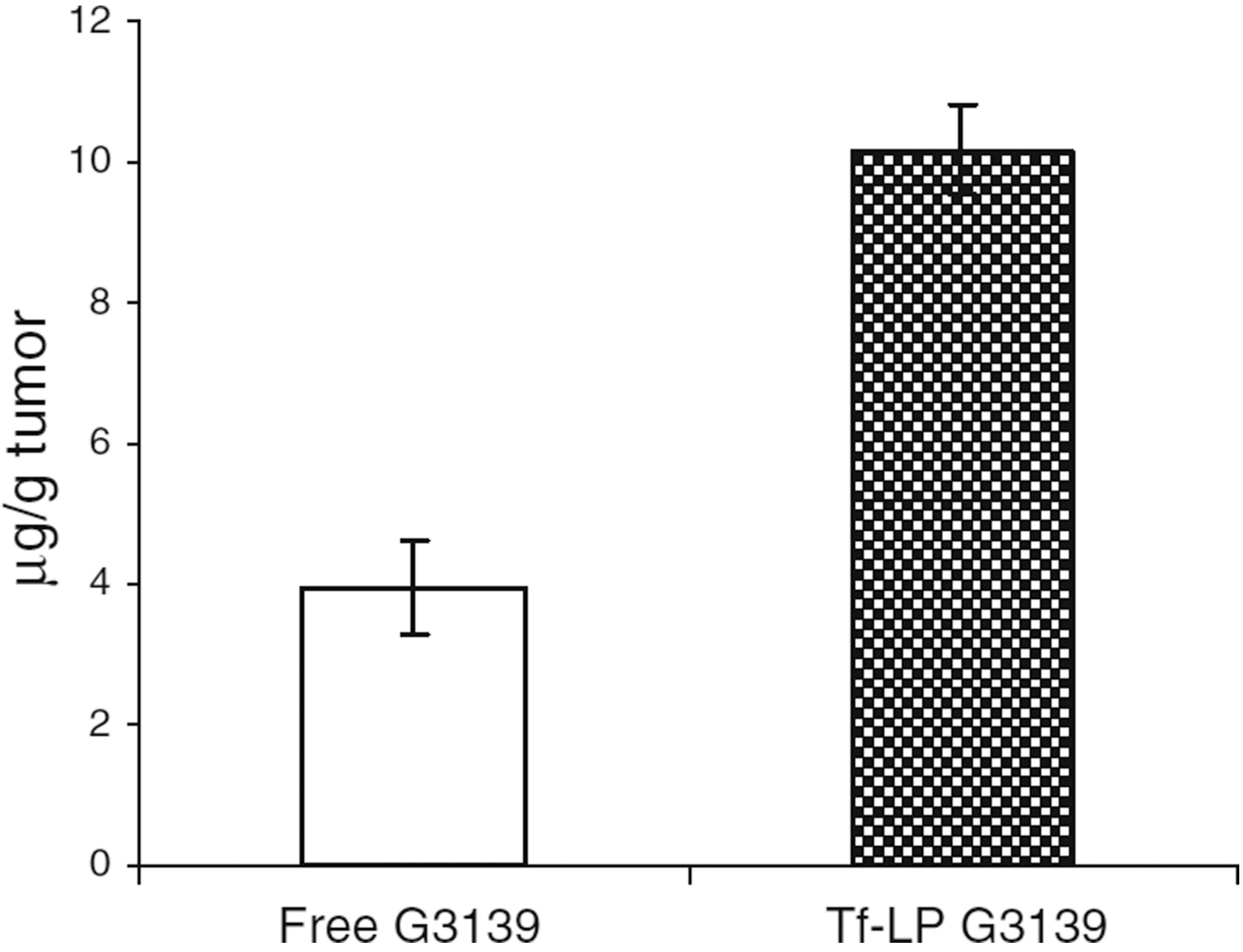

Fig. 2.

Tumor uptake of free and nanoparticle-loaded G3139. Tumor-bearing mice were given 5 mg/kg of free or Tf-LP-loaded G3139. Tumor tissues were harvested at 36 h postinjection and analyzed as described in the “MATERIALS AND METHODs” section (n=5).

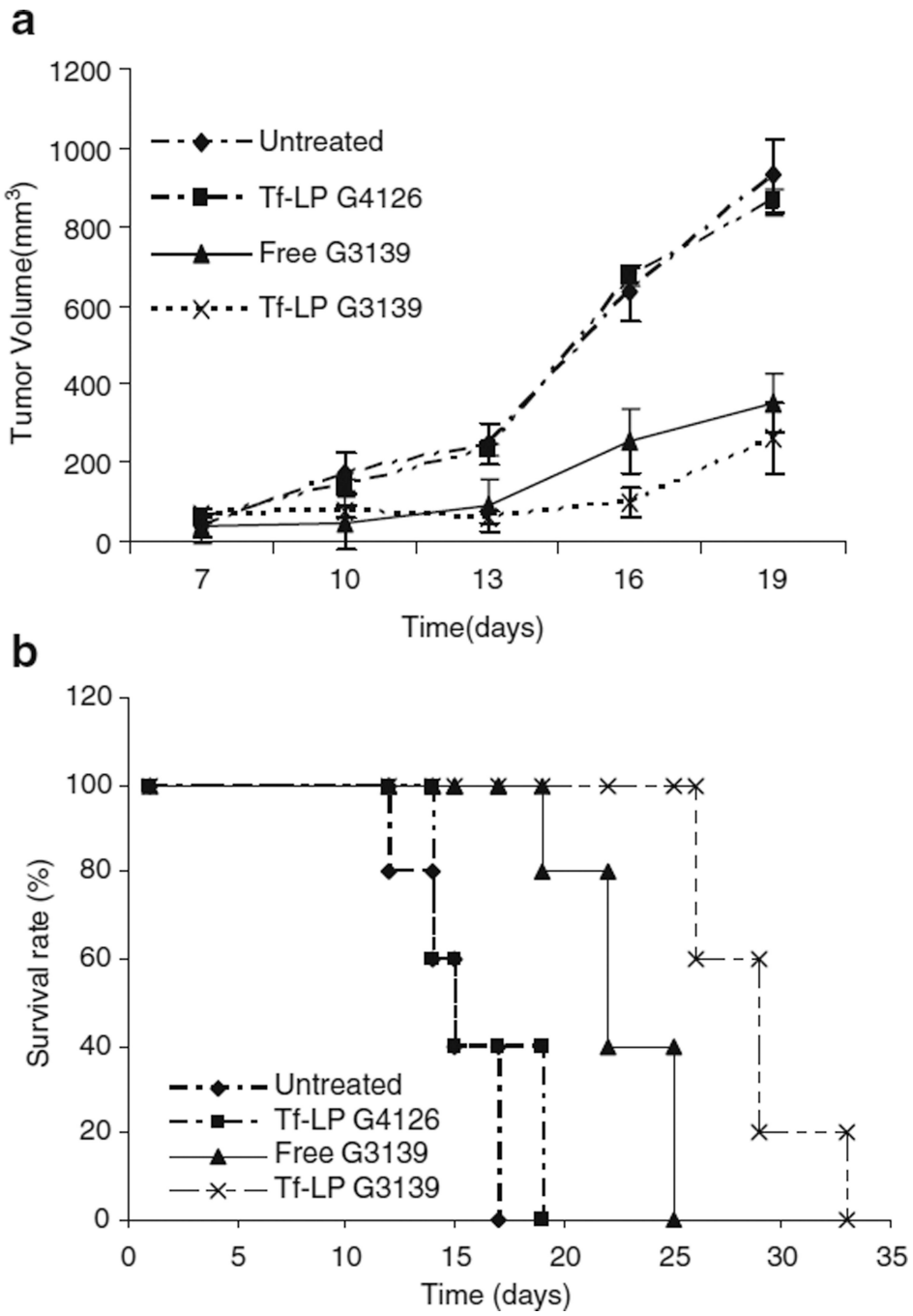

Fig. 3.

Antitumor activities of free and nanoparticle formulations of ODNs. **a** Effect of ODN therapy on growth of K562 xenograft tumors in nude mice. Tf-LP or free G3139 (5 mg/kg) was administered i.v. every other day starting on day 7 for a total of seven treatments. Tumor volume was monitored and plotted. **b** Effect of ODN therapy on survival of tumor-bearing nude mice. Nude mice (n=5) were untreated or injected i.v. with Tf-LP G4126, free G3139, or Tf-LP G3139.

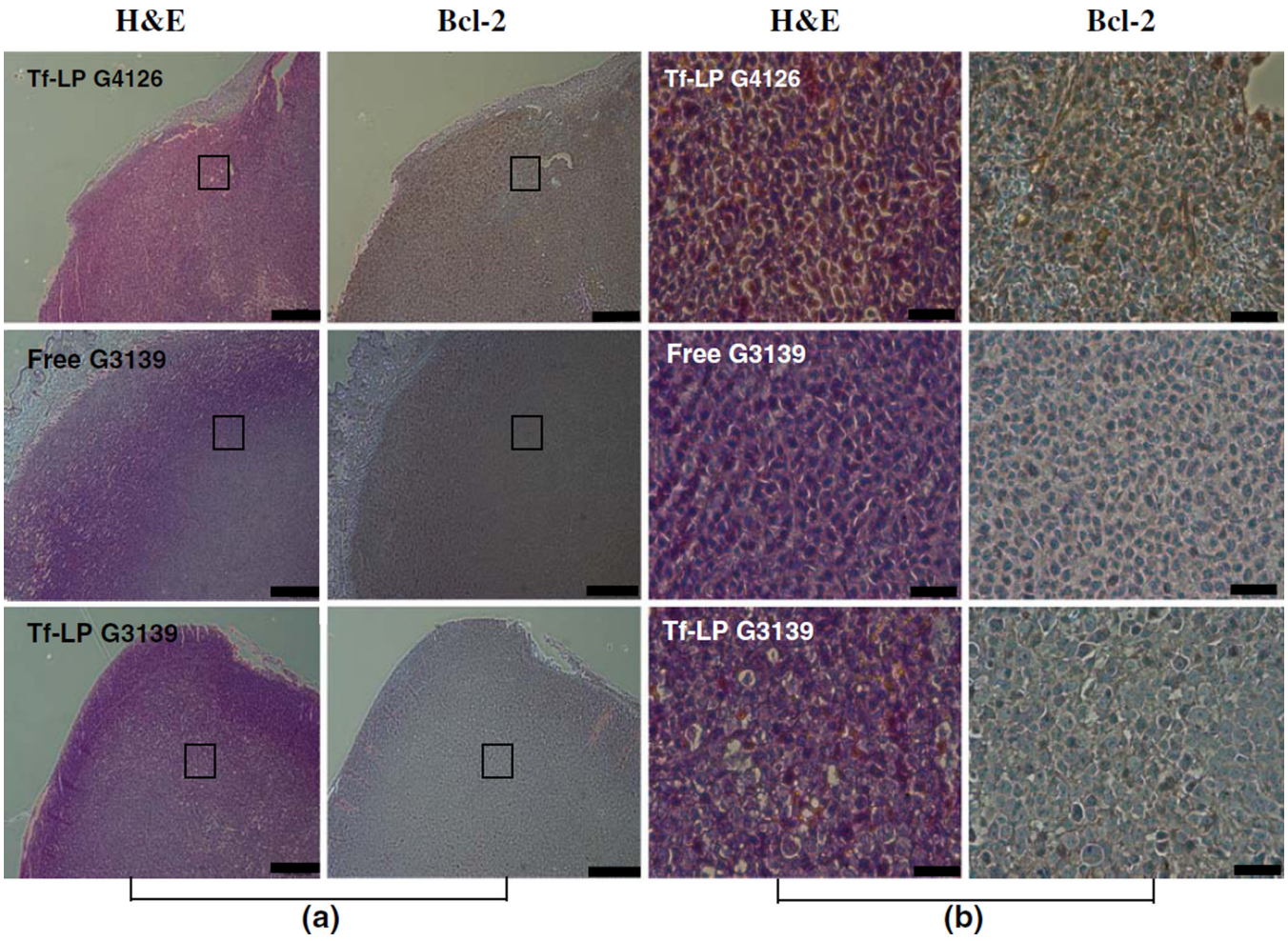

Fig. 4.

Bcl-2 expression in K562 xenograft tumors following ODN therapy. The tumor-bearing nude mice were untreated or treated every other day with i.v. injection of 5 mg/kg of Tf-LP G4126, free G3139, or Tf-LPG3139, starting on day 7 for a total of seven treatments. On day 15, two mice from each group were sacrificed. The tumor samples were then collected, fixed in formalin, embedded in paraffin and subjected to staining. **a** Low magnification images of the tumor sections; Scale bar: 300 μm. **b** Enlarged views of selected areas of (**a**). Scale bar: 60 μm.

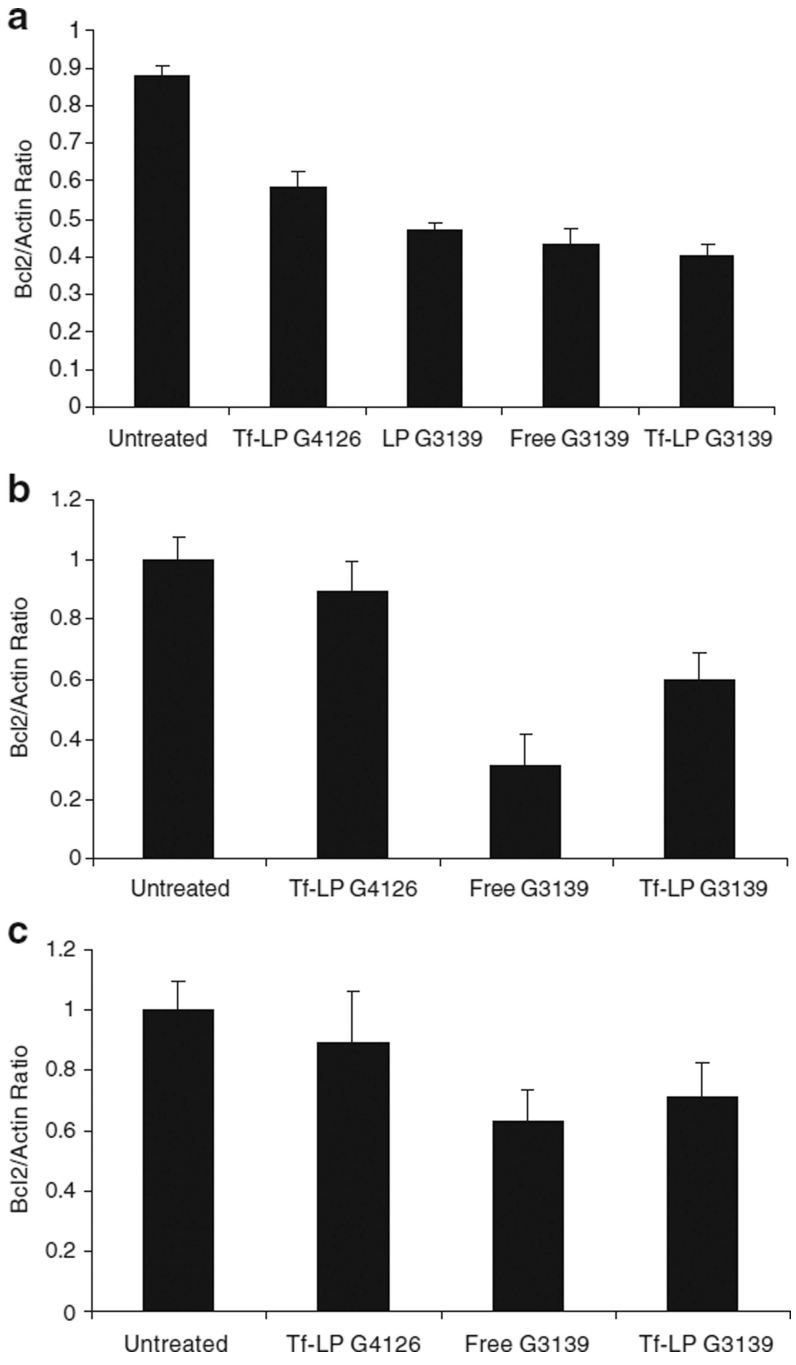

Fig. 5.

Bcl-2 downregulation by ODN in K562 cells *in vitro* and in xenograft tumors. **a** Bcl-2 expression in K562 cells (*in vitro*) that were untreated, or treated with 1 μM of various ODN formulations, determined by Western blot at 6 h. **b** Bcl-2 expression in K562 tumors that were untreated, or treated with i.v. injection of 5 mg/kg of various ODN formulations every other day starting on day 7 for a total of seven treatments. Bcl-2 expression was determined at 36 h after the last treatment by Western blot. **c** Bcl-2 expression in K562 cell clusters that were untreated or treated with free G3139, Tf-LP G3139, or Tf-LP G4126. Bcl-2 expression was determined at 6 h by Western blot.

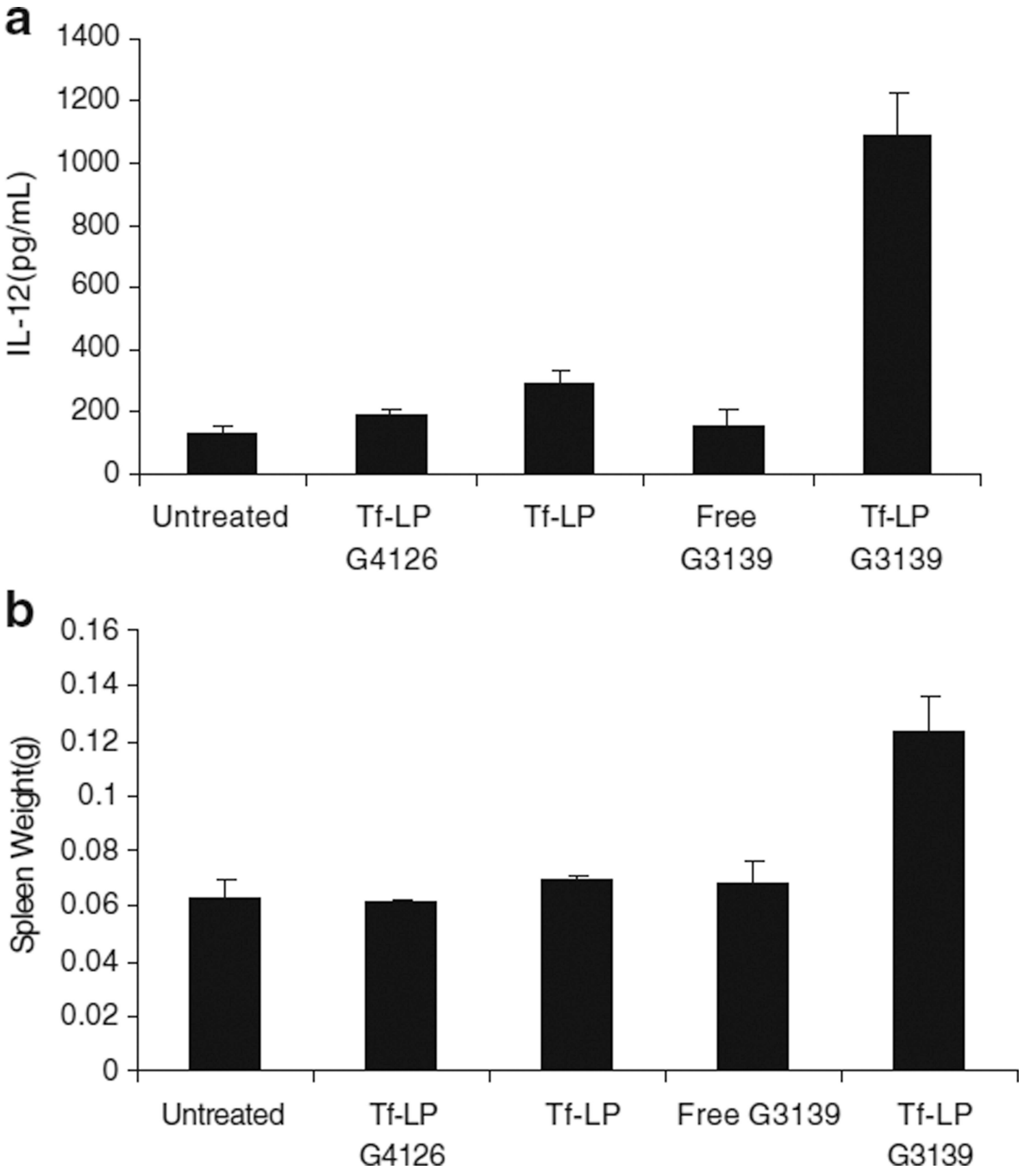

Fig. 6.

Immunomodulatory effects of ODN and ODN nanoparticles in tumor-bearing nude mice. **a** Induction of IL-12 expression. For the study, 6–8 week old nude mice bearing K562 tumor were untreated or given 5 mg/kg of various ODN formulations by tail vein injection. IL-12 levels were measured by ELISA, as described in the “MATERIALS AND METHODs” section. **b** Spleen weights for nude mice (n=5) that were untreated or treated with various ODN formulations or empty liposomes (Tf-LP).

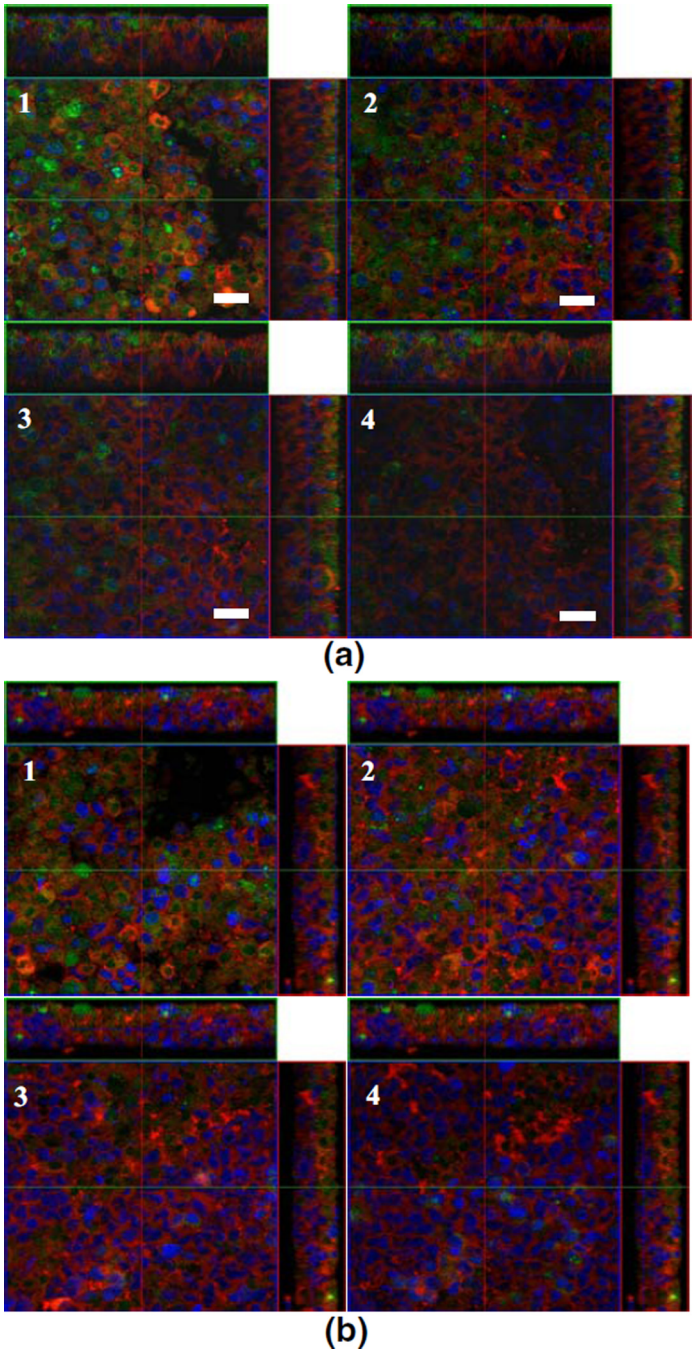

Fig. 7.

Confocal fluorescence images of K562 cell clusters treated with free G4243 or Tf-LP G4243. The cell clusters were treated with 1 μM of free G4243 or Tf-LP G4243 for 6 h and then fixed with 4% paraformaldehyde and stained with DiI and DRAQ5. They were imaged on a laser scan confocal microscope with excitation wavelengths of 488 nm and 543 nm for G4243 and DiI, respectively. The cytoplasm and nuclei were stained with red (DiI) and blue (DRAQ5), respectively. Green fluorescence was derived from FITC-labeled G3139 (G4243), thus indicates the distribution of the ODN within the cell clusters. The images show selected optical sections from the outer layers of cell cluster to the inner layers (from

1–4) **a** K562 cell cluster treated with free G4243. **b** K562 cell cluster treated with Tf-LP. Scale bar=20 μm.

Table I

Physical Chemical Characteristics of LP Formulations

Formulation	Particle size(nm)	Zeta-potential(mV)
Tf-LP G3139	141.3±2.0	3.6±2.9
LP G3139	126.8±2.2	11.6±3.6

Table II

Pharmacokinetic Parameters of Free and Tf-LP G3139

Parameters	Unit	Free G3139	Tf-LP G3139
C_{max}	μg/ml	61.1±5.5	29.3±2.01
$t_{1/2\beta}$	h	0.63±0.23	8.49±0.67
V_{ss}	ml/kg	0.22±0.15	0.64±0.18
CL	ml/kg/h	0.54±0.17	0.06±0.01
AUC	h μg/ml	9.33±0.97	90.02±8.94

C_{max} peak plasma concentration, $t_{1/2}$ half-life, V_{ss} steady-state volume of distribution, CL clearance, AUC area under the curve